http://dx.doi.org/10.5665/sleep.3422

Decreased Connectivity between the Thalamus and the Neocortex during Human Nonrapid Eye Movement Sleep

Dante Picchioni, PhD[1]; Morgan L. Pixa[1,2]; Masaki Fukunaga, PhD[3]; Walter S. Carr, PhD[4]; Silvina G. Horovitz, PhD[3]; Allen R. Braun, MD[4]; Jeff H. Duyn, PhD[3]

[1]Behavioral Biology Branch, Walter Reed Army Institute of Research, Silver Spring, MD; [2]Computer Systems Laboratory, Thomas Jefferson High School for Science and Technology, Alexandria, VA; [3]Advanced MRI Section, National Institute of Neurological Disorders and Stroke, Bethesda, MD; [4]Language Section, National Institute on Deafness and Other Communication Disorders, Bethesda, MD

Study Objectives: To determine whether thalamocortical signaling between the thalamus and the neocortex decreases from wakefulness to nonrapid eye movement (NREM) sleep.

Design: Electroencephalography and functional magnetic resonance imaging data were collected simultaneously at 02:30 after 44 h of sleep deprivation.

Setting: Clinical research hospital.

Participants: There were six volunteers (mean age 24.2 y, one male) who yielded sufficient amounts of usable, artifact-free data. All were healthy, right-handed native English speakers who consumed less than 710 mL of caffeinated beverages per day. Psychiatric, neurological, circadian, and sleep disorders were ruled out by reviewing each patient's clinical history. A standard clinical nocturnal polysomnogram was negative for sleep disorders.

Interventions: N/A.

Measurements and Results: A functional connectivity analysis was performed using the centromedian nucleus as the seed region. We determined the statistical significance of the difference between correlations obtained during wakefulness and during slow wave sleep. Neocortical regions displaying decreased thalamic connectivity were all heteromodal regions (e.g., medial frontal gyrus and posterior cingulate/precuneus), whereas there was a complete absence of neocortical regions displaying increased thalamic connectivity. Although more clusters of significant decreases were observed in stage 2 sleep, these results were similar to the results for slow wave sleep.

Conclusions: Results of this study provide evidence of a functional deafferentation of the neocortex during nonrapid eye movement (NREM) sleep in humans. This deafferentation likely accounts for increased sensory awareness thresholds during NREM sleep. Decreased thalamocortical connectivity in regions such as the posterior cingulate/precuneus also are observed in coma and general anesthesia, suggesting that changes in thalamocortical connectivity may act as a universal "control switch" for changes in consciousness that are observed in coma, general anesthesia, and natural sleep.

Keywords: Electroencephalography, functional connectivity, functional magnetic resonance imaging, neocortex, nonspecific nuclei, sleep, thalamus

Citation: Picchioni D; Pixa ML; Fukunaga M; Carr WS; Horovitz SG; Braun AR; Duyn JH. Decreased connectivity between the thalamus and the neocortex during human nonrapid eye movement sleep. *SLEEP* 2014;37(2):387-397.

INTRODUCTION

Connectivity between the thalamus and the neocortex underlies several fundamental processes, including relay of sensory signals during wakefulness[1] and increased sensory awareness thresholds during sleep.[2] These two processes depend on modality-specific thalamic nuclei that relay signals from sensory organs to corresponding primary sensory cortex and nuclei that transmit signals from the reticular activating system to the entire neocortex, respectively. Neurons in the latter category of nuclei (here indicated with the somewhat controversial adjective "nonspecific nuclei"[3]) are thus well suited to mediate changes in sensory awareness thresholds during sleep.

Sensory awareness thresholds progressively increase from wakefulness to light sleep (stages 1 and 2) and from light sleep to slow wave sleep (stages 3 and 4).[4] Such increases are associated with parallel changes in firing patterns of nonspecific thalamocortical neurons: in light sleep, nonspecific thalamocortical neurons are hyperpolarized by gamma-aminobutyric acidergic neurons located in the thalamic reticular nucleus. The discharge pattern of thalamocortical neurons initially changes from tonic to phasic, which results in generation of sleep spindles.[5] In slow wave sleep, thalamocortical neurons are further hyperpolarized. As a result of this additional hyperpolarization, the thalamus and the neocortex become functionally disconnected.[6,7] During slow wave sleep, the number of slow waves is positively correlated with sensory awareness thresholds.[8] These findings suggest that the thalamus acts as a "gate" where sensory signals are blocked from being transmitted to the neocortex.

With the exception of a single-participant analysis[9] and one investigation that was conducted in the context of other substantive questions on small-world networks,[10] to date, virtually all investigations of thalamocortical connectivity during sleep have been conducted in animals—and generally *in vitro*. Therefore, we sought to determine whether thalamocortical connectivity also decreases during nonrapid eye movement (NREM) sleep in humans. To address this issue, concurrent measurement of functional magnetic resonance imaging (fMRI) and electroencephalography (EEG) was performed to determine functional connectivity between the centromedian nucleus (the largest nonspecific thalamic nucleus) and the neocortex during wakefulness and NREM sleep.

Submitted for publication March, 2013
Submitted in final revised form July, 2013
Accepted for publication September, 2013

Address correspondence to: Dante Picchioni, PhD, National Institutes of Health, NINDS/NIMH, 10 Center Dr., Bethesda, MD 20892; Tel: (301) 451-9918; Fax: (301) 480-2558; E-mail: dante.picchioni@nih.gov

METHODS

Participants and Procedure

Procedures were approved by institutional review boards at the Walter Reed Army Institute of Research and the National Institutes of Health. All participants gave written informed consent and were monetarily compensated. Other results from the current study are published elsewhere.[11,12]

Participants ($n = 6$, age 24.2 ± 1.8 y, one male) were healthy, right-handed native English speakers who consumed less than 710 mL of caffeinated beverages per day (281 ± 243 mL), were nontobacco users and did not use any illicit drugs (verified by urine drug screen). Results of a urine pregnancy screen administered to the females immediately prior to beginning the laboratory phase of the study were negative. Participants did not engage in shift work for 12 mo prior to participation. Psychiatric, neurological, circadian (e.g., extreme morning or evening types), and sleep disorders were ruled out by reviewing each patient's clinical history. A clinical audiological examination was negative for auditory abnormalities. A standard clinical nocturnal polysomnogram (PSG; i.e., EEG, electro-oculography [EOG], submental electromyography [EMG], electrocardiogram, nasal/oral thermister respiratory flow, strain gauge thoracic and abdominal respiratory effort, snoring microphone, pulse oximetry, and anterior tibialis electromyography [EMG]) was negative for sleep disorders. Sleep was monitored at home using wrist actigraphs (Ambulatory Monitoring, Inc., Ardlsey, NY, USA) for 7 days prior to participation to ensure a regular sleep schedule (i.e., no incidents of spending 2 h or more of sleep time outside of reported sleep time) and adequate sleep (i.e., no less than reported daily sleep need).

To facilitate sleep inside the scanner, participants underwent approximately 44 h of total sleep deprivation during which they were under near-constant supervision and were not allowed stimulants (verified by controlling dietary intake). Participants were scanned at 02:30. The session lasted up to 3 h and consisted of multiple runs (i.e., separate fMRI scans) for some participants. The initial dataset contained 22 runs from 12 participants. Six participants were excluded because the associated data contained artifact or the participant did not exhibit a continuous bout of at least 5 min of stage 2, 3, and 4 sleep, of which at least 64% was stage 3 or 4 sleep (within the slow wave sleep bouts that met criteria, fMRI volumes with stage 2 were excluded in the final slow wave sleep analysis). Therefore, the final dataset contained six participants.

EEG Acquisition

PSG data were acquired using MRI-compatible hardware and associated software (Brain Products, GmbH, Gilching, Germany). The hardware included an alternating-current (AC) amplifier (BrainAmp MR Plus), a direct-current (DC) amplifier (BrainAmp ExG MR), and sintered silver-silver chloride ring electrodes (BrainCap MR). Data from a total of 16 channels were collected using the AC amplifier sampling at 5 kHz. Fourteen channels were used for scalp EEG, one channel for EOG, and one channel for electrocardiography. All electrodes were programmed to use FC_Z as the recording reference and a location near C_Z as the ground. Chin EMG data were collected using the DC amplifier. The acquisition software used was Brain Products' Recorder software.

Respiratory effort was measured using respiratory bellows on the abdomen, and cardiac rate was measured using an infrared pulse oximeter on a finger. Both transducers were standard equipment for the MRI scanner; data were collected using custom software at a sampling rate of 1 kHz.

EEG Processing

fMRI gradient field switching and static field ballistocardiographic artifacts were removed using routines in Brain Products' Analyzer software. These routines are based on standard approaches for EEG data collected during fMRI.[13,14] All subsequent EEG data processing also was performed using Analyzer.

Sleep scoring was conducted by adapting the standard criteria as explained as follows[15]: a band-pass filter of 0.5-20.0 Hz for EEG and EOG channels and a high-pass filter of 10 Hz and a low-pass filter of 70 Hz with a notch filter at 60 Hz for the EMG channel. Modifications to the standard sleep scoring were as follows. Sleep scoring was performed from C_3 with a P_3 reference rather than the standard A_2 reference because the A_2 reference caused amplification of the EEG signal due to the static magnetic field. Sleep was scored in 12-sec epochs so that 4 rather than 10 fMRI volumes would be included in each epoch. In effect, this maximized the temporal resolution of the EEG signal and made it more comparable to the temporal resolution of the fMRI signal. All records were scored by an experienced PSG technologist. Interrater reliability for a representative record between this scorer and a diplomate of the American Board of Sleep Medicine was 73% (which was considered acceptable given the amount of artifact contained in the records).

MRI Acquisition

MRI data were acquired on a 3T scanner (GE, Milwaukee, WI, USA). For the functional runs, a 16-channel receive-only detector array was used.[16] This array is designed with a helmet-type construction that minimizes the distance between the individual coils and the scalp as a tradeoff for slight signal dropout in the lower cerebellum and brainstem. Blood oxygen level- dependent (BOLD) fMRI was implemented using an echo planar imaging sequence. This step was preceded by a short functional run that included 10 different echo times, to be used as a reference for correction of geometric distortions. Functional runs included 25 axial slices (3.45×3.45 mm^2 nominal in-plane resolution, 4.5 mm thickness, 0.5 mm gap). Other parameters were as follows: repetition time = 3 sec, echo time = 45 ms, flip angle = 90°, and a maximum of 3,600 fMRI volumes. To facilitate sleep, acoustic noise generated by the functional sequence was kept below a sound pressure level of 96 decibels by decreasing the bandwidth to 62.54 kHz and limiting the gradient slew-rate to 25 T/m/sec. Participants also wore earplugs.

T2-weighted anatomical data (fast spin echo) were collected for geometric distortion correction. If the session was interrupted and the participant agreed to continue, an additional set of T2-weighted anatomical data were acquired to correct for the new head position.

T1-weighted anatomical data (magnetization prepared rapid gradient echo) were collected to identify and trace the centromedian nucleus and to aid registration to a standard anatomical template. These data were collected in a separate session on another 3T scanner in the same facility using the following parameters: axial plane, echo time = 2.5 ms, flip angle = 6°, field of view = 250 mm, matrix = 256 × 256, slice thickness = 1.2 mm, and 146 slices.

MRI Processing

Data were preprocessed using custom routines written in Interactive Data Language (ITT Visual Information Solutions, Inc., Boulder, CO, USA) unless otherwise indicated. Slice timing correction was applied. Motion correction was applied by registering the functional data to the first volume of the short functional run. Both corrections were performed using SPM2 software (Wellcome Department of Cognitive Neurology, London, UK). Distortion correction was performed using the field map computed from the 10 different echo times of the short functional run.[17] This correction was necessary because of the geometric distortions caused by the low bandwidth needed to decrease the acoustic noise associated with gradient switching. Remaining distortion was corrected by nonlinearly deforming the functional data to match the undistorted T2-weighted anatomical data (AIR 5.2.5 software, University of California, Los Angeles, Los Angeles, CA, USA). Physiological noise was corrected by modeling cardiac rate, respiratory rate, and respiratory envelope and regression of activity associated with these variables.[18,19] Global signal correction was applied using the within-volume mean as a linear regression covariate. A high-pass filter (0.005 Hz) was applied to remove baseline drift.

The following additional processing steps were performed using Analysis of Functional NeuroImages (AFNI, National Institute of Mental Health, Bethesda, MD, USA): the centromedian nucleus of the thalamus was manually traced in native space in the coronal plane using the T1-weighted anatomical data from each participant (Figure 1). The procedure for manually tracing the centromedian nucleus was as follows. Tracing was performed in native space on coronal images from anterior to posterior using a neuroanatomy atlas as a supplemental guide.[20] The beginning of the centromedian nucleus was confirmed by using the appearance of the red nucleus in the midbrain as a landmark. Tracing was performed so that the centromedian nucleus was always inferior to the medial dorsal nucleus and always superior (with a small gap that consisted of the thalamic fasciculus) to the red nucleus. The end of the centromedian nucleus was confirmed by using the appearance of the posterior commissure as a landmark.

The left and right portions of the centromedian nucleus were included in the same region of interest. After tracing, the dataset was converted to the resolution of the functional data with erosion for partial volume correction (Figure 1). Functional data for each participant was registered with the T1-weighted anatomical data. The average raw BOLD signal of all voxels in the region of interest was then exported for use in the connectivity correlations. Finally, the functional data were blurred to a specified full width at half maximum smoothness of 4 mm using a gaussian spatial blurring.

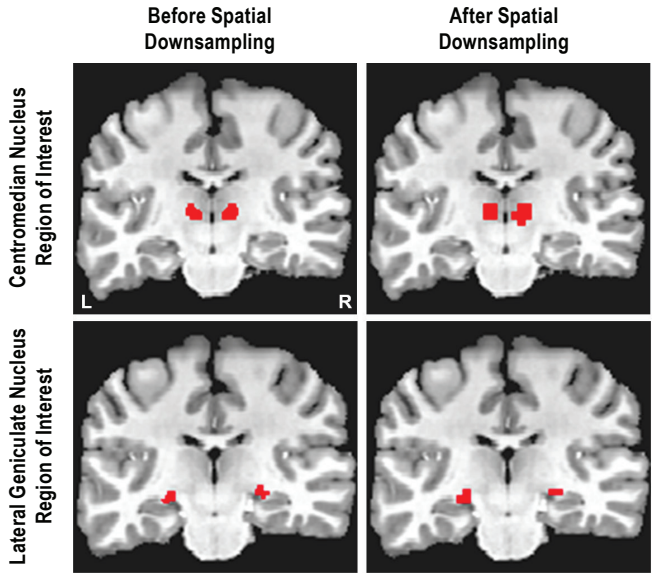

Figure 1—The regions of interest for a single participant before and after conversion to the resolution of the functional data.

Analysis

For the slow wave sleep condition, a continuous bout of at least 5 min of stage 2, 3, or 4 was chosen from the end of the NREM portion of the first sleep cycle, when spectral power in the 0.5-4.0 Hz band is at its highest[21] and when sensory awareness thresholds also are highest.[8] Within the slow wave sleep bouts that met criteria, fMRI volumes with stage 2 were excluded in the final slow wave sleep analysis. For the wake condition, at least 5 min of PSG-defined wakefulness was chosen from fMRI volumes that were distributed throughout the entire run. Hypnograms showing temporal placement of fMRI volumes chosen for the bouts of slow wave sleep and wakefulness are presented in Figure 2. In one participant, all of the epochs that were chosen for the wake condition occurred after the slow wave sleep bout. However, across all participants, an average of 35% ± 30% of the epochs that were chosen for the wake condition occurred before the slow wave sleep bout. The amount of sleep and wakefulness was equalized; whichever value was smaller determined the total data for each condition for that participant. For example, if a participant accumulated 10 min of slow wave sleep but 20 min of wakefulness, then only half of the available wakefulness in the run was used. The mean amount of data across participants was 6.2 ± 3.2 min or 123 ± 63 fMRI volumes of stage 3 or 4 sleep. The average length of the bouts of wakefulness was 39.10 ± 30.03 sec, and the average length of the bouts of slow wave sleep was 125.75 ± 109.00 sec; this difference was not significant ($t(5) = 1.60$, $P = 0.17$).

All statistical analyses were performed using AFNI. The analyses were performed according to the standard two-level approach at the individual participant and group level. For each participant, the average raw BOLD signal extracted from voxels in the centromedian nucleus was correlated with all voxels in the brain while controlling for motion with the six motion parameters obtained from the earlier motion correction. This correlation was calculated twice, once for the slow wave sleep

condition excluding all other volumes in the run and similarly for the wake condition.

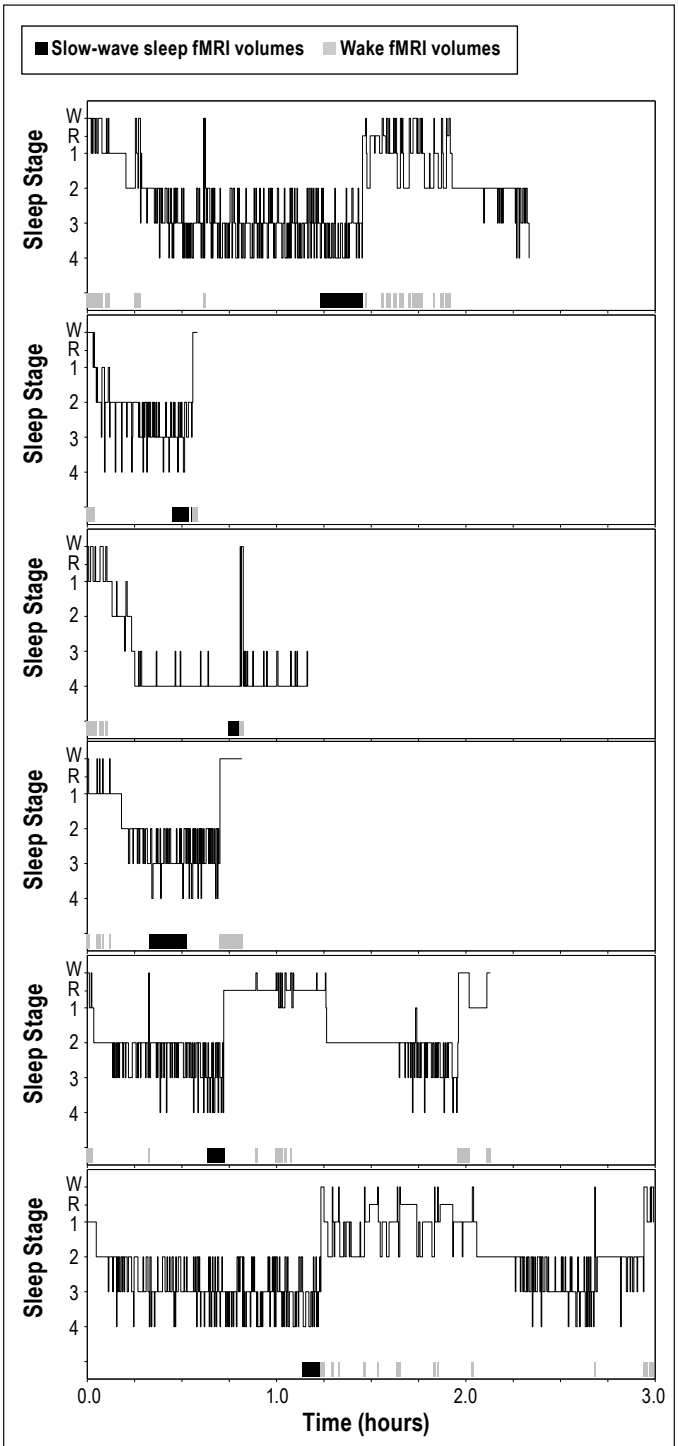

Figure 2—Electroencephalography sleep staging and functional magnetic resonance imaging (fMRI) volume selection. For the slow wave sleep condition, a continuous bout of at least 5 min of stage 2, 3, or 4 was chosen from the end of the nonrapid eye movement portion of the first sleep cycle, when spectral power in the 0.5-4.0 Hz band is at its highest[21] and when sensory awareness thresholds also are highest.[8] Within the slow wave sleep bouts that met criteria, fMRI volumes with stage 2 were excluded in the final slow wave sleep analysis. For the wake condition, at least 5 min of polysomnography-defined wakefulness was chosen from fMRI volumes that were distributed throughout the entire run. W = Wakefulness and R = REM.

Correlations were then transformed using the Fisher *z*-transformation. The statistical significance of the difference between the transformed sleep and wake correlations was calculated with a *z* test that uses a pooled standard error for the two correlations:

$$z = \frac{z'_S - z'_W}{\sqrt{1/(n_S - 3) + 1/(n_W - 3)}}$$

The absolute value for each transformed correlation was used when calculating the significance of the difference between the two correlations. Absolute values were used because differences in the magnitude of thalamocortical connectivity were of interest regardless of direction. For example, a strong positive correlation during wakefulness and a strong negative correlation during sleep would still indicate the same magnitude of connectivity—and thus the difference between wake and sleep conditions would be zero.

If both individual correlations were not significant, the corresponding voxel was excluded from further analysis. This prevented the situation in which neither correlation was significant, but they were significantly different from each other. However, if for example a correlation was significantly positive during wakefulness but not significant during sleep, then that voxel would still be included.

The aforementioned analysis steps represent the first level of the standard two-level approach in neuroimaging research: the individual-participant level. The dataset was then transformed into Talairach space using a standardized template (Wellcome Department of Cognitive Neurology, London, UK) with a final voxel size of 3.44 mm^3. The *z* scores were then averaged across participants. This resulted in a group average *z* map. These values were tested for significance ($P < 0.05$) using a *t* test with a null value of zero. This represents the second level of the standard two-level approach in neuroimaging research: the group level. The results are displayed on the standardized average of 27 T1-weighted runs of a single participant known as the Colin Brain (Montreal Neurological Institute, Montreal, Canada). Significant voxels outside the brain were masked out of these images.

Coordinates in Talairach space (left/right, posterior/anterior, inferior/superior, negative/positive convention) that were reported were determined by the maximal *t* value (or minimal for negative values) within each cluster of significant voxels. Significant voxels outside of the neocortex were excluded to focus specifically on neocortical areas. Multiple testing correction was subsequently applied at the group level using the neocortical region of interest as the input mask. Using an individual voxel probability threshold of $P < 0.05$ in the context of Monte Carlo simulations that are implemented within AFNI, we determined that clusters ≥ 28 voxels would have a whole-volume probability threshold of $P < 0.05$. Clusters less than 28 voxels were therefore excluded. Anatomical regions associated with peaks in each cluster were determined using the Talairach Daemon.[22]

Supplementary Analyses

To examine the specificity of changes in connectivity to slow wave sleep, the analysis was repeated for stage 2 sleep. fMRI

volumes that coincided with stage 2 sleep were chosen from the beginning of the NREM portion of the first sleep cycle. We limited the number of stage 2 epochs so that the total data in this analysis equaled the total data from the slow wave sleep analysis. In addition to comparing connectivity during stage 2 sleep to connectivity during wakefulness, we also compared connectivity during stage 2 sleep to connectivity during slow wave sleep.

The relatively large functional voxel size compared to the size of the anatomical region raises the concern that the region of interest is not capturing the unique functional activity of the centromedian nucleus. In other words, a whole-thalamus region of interest might provide the same results. Therefore, another region of interest was created for a nearby thalamic nucleus: the lateral geniculate nucleus (Figure 1). The procedure for manually tracing the lateral geniculate nucleus was as follows. Tracing was performed in native space on coronal images from anterior to posterior using a neuroanatomy atlas as a supplemental guide.[20] The beginning of the lateral geniculate nucleus was confirmed by noting when the putamen began to transform into the discontinuous striatal cell bridges and when the most posterior portion of the insula was still clearly visible. Tracing was performed so that the lateral geniculate nucleus was superior (with a small gap that consisted of the hippocampal sulcus) to the most medial portion of the hippocampus. The end of the lateral geniculate nucleus was confirmed by using the most posterior portion of the putamen and insula as a landmark.

Suitability of the lateral geniculate nucleus for use as a control region requires it to have a roughly similar size and signal-to-noise ratio as the centromedian nucleus. This was confirmed as follows. At the same processing step where the average values in each region of interest were exported (i.e., before spatially blurring the functional data), we calculated the temporal signal-to-noise ratio for each region of interest for one participant. The average values were similar for the centromedian nucleus (118 ± 37) and the lateral geniculate nucleus (108 ± 50). These calculations were performed for another region as well (the primary visual cortex), and the obtained values were again similar (90 ± 41). We also calculated the average bilateral volume of each region of interest across participants. This was performed immediately after the processing step where we spatially downsampled the region-of-interest masks to the resolution of the functional data. The region of interest for the lateral geniculate nucleus was smaller (419.7 ± 71.2 mm^3) than the region of interest for the centromedian nucleus (528.0 ± 282.6 mm^3), but this difference was not significant ($t(5) = 0.85$, $P = 0.22$).

The left and right portions of the lateral geniculate nucleus were included in the same region of interest. The aforementioned primary analysis was repeated with the exception that behavioral state was held constant by only examining wakefulness; the comparison was instead between the correlations for each seed region. A unique connectivity pattern for each seed region would suggest that the spatial resolution of the functional data is sufficient to distinguish between individual thalamic nuclei. The other differences between this analysis and the primary analysis were that we did not mask subcortical voxels and we did not use absolute values of the correlations.

Table 1— Average min of each sleep stage for the entire run (n = 6)

	M	SD
Wake	8.6	2.3
N1	12.6	8.2
N2	39.4	25.3
N3	23.4	17.6
S4	15.6	18.6
REM	7.5	11.0
Total	107.1	50.1

M, mean; REM, rapid eye movement; SD, standard deviation.

The difference in connectivity for the lateral geniculate nucleus from wakefulness to slow wave sleep was also calculated as a negative control. The aforementioned primary analysis was repeated with the exception that the lateral geniculate nucleus was used as the seed region. If the decreases in connectivity are unique to nonspecific nuclei, then there should be no differences in connectivity between this nucleus and its corresponding region of primary sensory cortex. The only other difference between this analysis and the primary analysis was that we masked all voxels except those in the calcarine cortex.

A final supplementary analysis was performed to determine the direction of change in correlations in slow wave sleep regardless of whether the absolute value of the difference was significant. This was performed by transforming the correlations at the group level rather than at the individual participant level. This necessitated reducing the sample size to the smallest number of volumes that was present in a participant. With these restrictions, 3.5 min or 70 fMRI volumes were used from each participant. All other procedures were identical to the primary analysis. Although the smaller sample size renders the two analyses incompletely comparable, some additional useful information can be obtained by categorizing the change in the correlations.

RESULTS

Average sleep data for the entire scanning session are presented in Table 1. These data represent sleep scoring before restricting the fMRI volumes to the distinct bouts of slow wave sleep and wakefulness. The values for the total min of each sleep stage are typical for sleep following a period of total sleep deprivation.

Statistically significant differences between wake and slow-wave sleep correlations are presented in Figure 3A. These images are from the point in the processing stream after group averaging but before masking subcortical voxels and applying the multiple testing correction. Nearly all significant changes in the correlations were decreases. To provide a graphical illustration of these changes, the change in the average r value within the largest cluster of significant decreases in connectivity is presented in Figure 3B. Correlations in the cingulate gyrus were negative during wakefulness and became less so during sleep.

Regions associated with the neocortical clusters of significant decreases in connectivity during slow wave sleep after

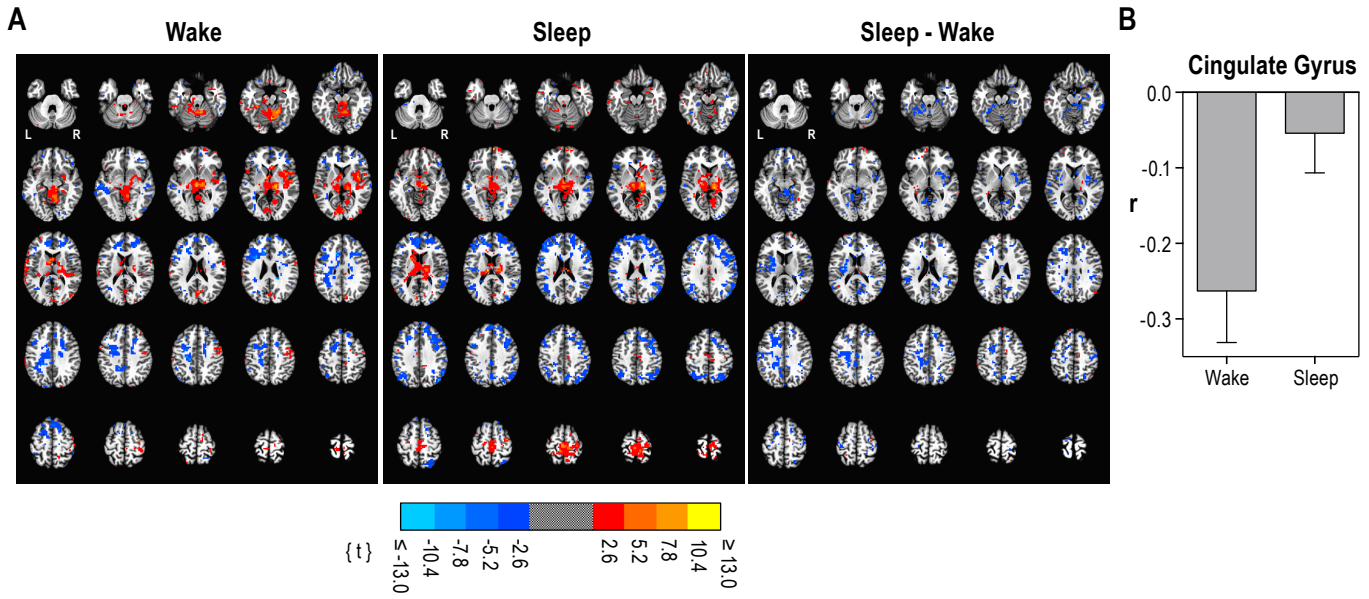

Figure 3—(A) Significance of the centromedian correlations during wakefulness, slow wave sleep, and the difference between the two. Maps were obtained after averaging across all participants but before masking subcortical voxels and applying the multiple testing correction. Maps are masked with an individual-voxel threshold of P < 0.05. Slices begin at Talairach coordinates in the z plane at 28I and end at 68S with a 4-mm gap. **(B)** Change in the average r value (mean ± standard deviation) within the largest cluster of significant decreases in connectivity from Table 2.

Table 2—Neocortical clusters of significant decreases in centromedian nucleus correlations from wakefulness to slow wave sleep

Region	Cluster size in voxels	Peak *t* score	x	y	z
Cingulate gyrus	83	-6.23	-16	-25	38
Precuneus	41	-4.46	29	-70	41
Medial frontal gyrus	33	-5.93	12	30	41

Coordinates in Talairach space (left/right, posterior/anterior, inferior/superior, negative/positive convention) were determined by the peak *t* score within the clusters of significant voxels from the neocortically masked dataset. Using an individual voxel probability threshold of P < 0.05 in the context of Monte Carlo simulations that are implemented within Analysis of Functional NeuroImages, we determined that clusters ≥ 28 voxels would have a whole-volume probability threshold of P < 0.05. Clusters less than 28 voxels were therefore excluded. Voxel size is 3.44 mm^3.

multiple testing correction are listed in Table 2. These neocortical regions were all heteromodal. In contrast to the three neocortical clusters of significant decreases, no neocortical clusters of significant increases were observed.

To examine the specificity of changes in connectivity to slow wave sleep, the analysis was repeated for stage 2 sleep. Regions associated with the neocortical clusters of significant decreases in connectivity during stage 2 sleep after multiple testing correction are listed in Table 3. Although more clusters of significant decreases were observed in stage 2 sleep, these results were similar to the results for slow wave sleep. All of the clusters of significant decreases that were observed during slow wave sleep were observed during stage 2 sleep. However, decreases in connectivity in, for example, the insula and in the parahippocampal gyrus were observed in stage 2 sleep but not in slow wave sleep. In contrast to the 16 neocortical clusters of significant decreases, no neocortical clusters of significant increases were observed. In addition to comparing connectivity during stage 2 sleep to connectivity during wakefulness, we also compared connectivity during stage 2 sleep to connectivity during slow wave sleep. Connectivity was actually lower in stage 2 sleep compared to slow wave sleep in three clusters: medial frontal gyrus (x = -2, y = -25, z = 62), middle temporal gyrus (x = 46, y = -60, z = 27), and middle frontal gyrus (x = -43, y = 30, z = 20).

To verify that the resolution of the functional data was sufficient to distinguish between individual thalamic nuclei, the aforementioned analysis was repeated for the lateral geniculate nucleus during wakefulness. Statistically significant differences between these correlations averaged across all participants are presented in Figure 4. The figure shows a binary dataset where a colored voxel indicates a significant difference. Numerous clusters of such significant differences were seen, including the cerebellum, thalamus, basal ganglia, prefrontal cortex, and other heteromodal regions. We also examined the centromedian and lateral geniculate correlation maps without any statistical thresholds, and each seed region also yielded a unique overall correlation pattern.

Table 3—Neocortical clusters of significant decreases in centromedian nucleus correlations from wakefulness to stage 2 sleep

Region	Cluster size in voxels	Peak *t* score	x	y	z
Superior temporal gyrus	96	-8.56	64	-12	0
Precuneus	93	-4.78	22	-67	48
Cingulate gyrus	90	-12.04	12	23	27
Cingulate gyrus	82	-6.32	-16	13	31
Insula	62	-9.41	-33	-22	17
Precentral gyrus	57	-6.34	-50	2	27
Middle frontal gyrus	50	-6.17	36	44	20
Fusiform gyrus	49	-6.48	-36	-39	-18
Parahippocampal gyrus	47	-7.19	19	-49	-4
Precentral gyrus	45	-4.43	40	-8	27
Cingulate gyrus	43	-7.55	-16	-36	38
Medial frontal gyrus	40	-6.41	-12	50	10
Transverse temporal gyrus	40	-4.89	36	-29	10
Middle frontal gyrus	31	-6.34	43	19	31
Cingulate gyrus	30	-6.79	12	-43	31
Middle frontal gyrus	29	-8.06	33	40	-11

Coordinates in Talairach space (left/right, posterior/anterior, inferior/superior, negative/positive convention) were determined by the peak *t* score within the clusters of significant voxels from the neocortically masked dataset. Using an individual voxel probability threshold of $P < 0.05$ in the context of Monte Carlo simulations that are implemented within Analysis of Functional NeuroImages, we determined that clusters ≥ 28 voxels would have a whole-volume probability threshold of $P < 0.05$. Clusters less than 28 voxels were therefore excluded. Voxel size is 3.44 mm^3.

To test whether the decreases in centromedian/neocortical connectivity during slow wave sleep are unique to nonspecific nuclei, we calculated the difference in lateral geniculate nucleus connectivity between wakefulness and slow wave sleep in the calcarine cortex. No clusters of significant voxels were observed.

To categorize the direction of change in correlations during slow wave sleep regardless of whether the absolute value of the difference was significant, Table 4 presents the 18 mutually exclusive categories that characterize the correlation in wakefulness, slow wave sleep, and the significance of the difference between the two. A "+" or "–" in one of the first two columns of the category label indicates a significantly positive or negative correlation in wakefulness or slow wave sleep, respectively. The third column indicates whether the difference between the two was significant. Although the smaller sample size from this supplementary analysis makes it difficult to compare it to the primary analysis, some additional useful information can be obtained. Most of the clusters of significant voxels were in categories without a significant difference between the two correlations. One of these categories consisted of voxels that began as significantly negative during wakefulness and became nonsignificant during sleep (category #11, Table 4). This is consistent with the largest cluster from the primary analysis.

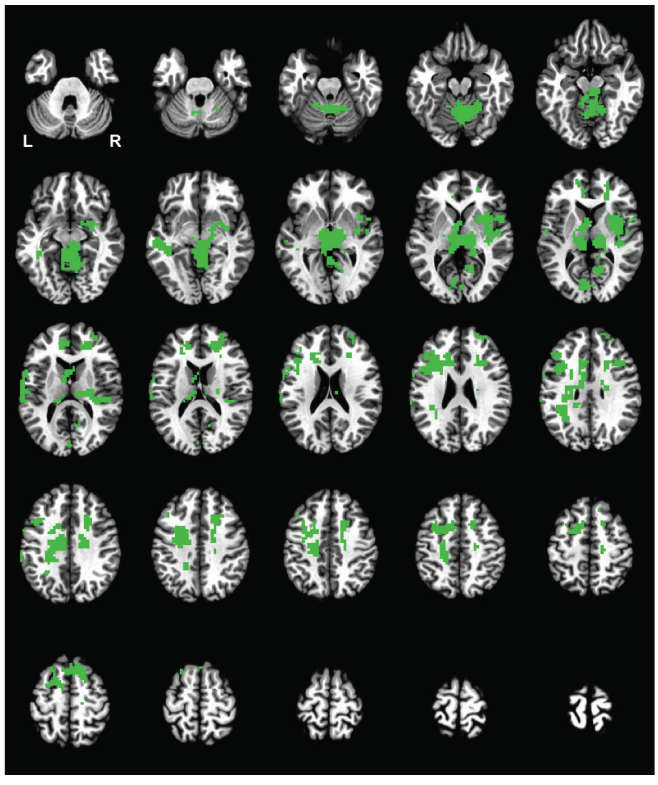

Figure 4—Statistical significance of the difference between the centromedian nucleus and lateral geniculate correlations during wakefulness when averaged across all participants. All significant differences ($P < 0.05$) are represented with a single color. Slices begin at Talairach coordinates in the z plane at 28I and end at 68S with a 4-mm gap.

DISCUSSION

In this study, we sought to answer the following question: does thalamocortical connectivity decrease during NREM sleep in humans? Based on the thalamocortical functional deafferentation observed in previous animal research, we hypothesized that a decrease in thalamocortical connectivity would

Table 4—Categorization of the change in connectivity from wakefulness to slow wave sleep

Categories (wake / sleep / difference)	Cluster size in voxels	x	y	z
1) + / + / from zero				
** NO CLUSTERS FOUND **				
2) + / + / ns				
** NO CLUSTERS FOUND **				
3) + / + / to zero				
** NO CLUSTERS FOUND **				
4) + / ns / ns				
Insula	60	43	-2	4
Postcentral gyrus	38	-57	-24	21
Precentral gyrus	37	53	-9	25
5) + / ns / to zero				
Transverse temporal gyrus	37	40	-28	13
6) + / – / ns				
** NO CLUSTERS FOUND **				
7) + / – / to zero				
** NO CLUSTERS FOUND **				
8) – / – / to zero				
** NO CLUSTERS FOUND **				
9) – / – / ns				
** NO CLUSTERS FOUND **				
10) – / – / from zero				
** NO CLUSTERS FOUND **				
11) – / ns / ns				
Medial frontal gyrus	45	-16	9	48
12) – / ns / to zero				
** NO CLUSTERS FOUND **				
13) – / + / ns				
** NO CLUSTERS FOUND **				
14) – / + / to zero				
** NO CLUSTERS FOUND **				
15) ns / + / ns				
Medial frontal gyrus	49	1	-24	61
16) ns / + / from zero				
** NO CLUSTERS FOUND **				
17) ns / – / ns				
Medial frontal gyrus	343	7	45	22
Inferior parietal lobule	157	-38	-39	43
Superior temporal gyrus	130	-46	-56	23
Middle frontal gyrus	128	43	19	29
Middle frontal gyrus	104	-35	37	24
Superior temporal gyrus	51	59	-33	13
Precuneus	51	4	-58	38
Superior parietal lobule	48	30	-54	48
Inferior frontal gyrus	34	-42	6	29
Postcentral gyrus	31	53	-24	35
18) ns / – / from zero				
** NO CLUSTERS FOUND **				

A "+" or "–" in one of the first two columns of the category label indicates a significantly positive or negative correlation in wakefulness or slow wave sleep, respectively. The third column indicates whether the difference between the two was significant; "to zero" indicates a significant change in the direction toward zero, and "from zero" indicates a significant change in the direction away from zero. Coordinates in Talairach space (left/right, posterior/anterior, inferior/superior negative/positive convention) were determined by the center of mass of the clusters of significant voxels from the neocortically masked dataset. Voxel size is 3.44 mm^3.

occur during NREM sleep. This hypothesis was supported, thus providing evidence of a functional deafferentation between the centromedian nucleus of the thalamus and the neocortex during NREM sleep in humans.

Comparisons with Previous Literature

Few studies have been designed to examine functional connectivity during sleep using fMRI, and the focus of most of these studies was corticocortical connectivity.[11,23,24] Consistently, results from these studies have shown that during slow wave sleep, corticocortical connectivity is disrupted. This is consistent with the decrease in corticocortical connectivity that was observed using EEG.[25] In that study, connectivity was defined as the propagation distance of a transcranial magnetic stimulation pulse. Results from these studies indicate that sleep is characterized by a decrease in neocortical integration, which may be the neurophysiologic basis of decreased consciousness during sleep.[26]

Equally important in understanding the neurophysiologic basis of consciousness is an understanding of changes in connectivity between neocortex and subcortical structures because connectivity changes in subcortical structures play a substantial role in regulating cortical arousal and sleep-wake states. Laufs and colleagues used a seed in the thalamus that was defined according to the activity associated with sleep spindles.[9] The investigators observed positive correlations in heteromodal cortical regions and negative correlations in primary cortical regions, and the correlations were not significantly different across sleep stages. Spoormaker and colleagues used fMRI to examine thalamocortical connectivity during sleep in the larger context of a 90-region, data-driven approach using graph theory.[10] Compared to wakefulness, cortical connectivity with the thalamus decreased in all NREM sleep stages, a finding that is consistent with the combined stage 2 and slow wave sleep findings from the current study. Therefore, it is important to note that changes in centromedian/neocortical connectivity may not be unique to slow wave sleep. Spoormaker and colleagues used the entire thalamus as the region of interest. In contrast, we identified and used the centromedian nucleus as an example of a nonspecific nucleus and the lateral geniculate nucleus as an example of a relay nucleus.

Interpretations and Implications

In animals, a functional deafferentation (decreased functional connectivity) exists between the thalamus and the neocortex during slow wave sleep. Decreases in centromedian/neocortical connectivity seen in the current study may be the human equivalent of this functional deafferentation. Does this decrease in centromedian/neocortical connectivity underlie increased sensory awareness thresholds during sleep? Although some unimodal cortical regions displayed decreased centromedian/neocortical connectivity in the current study, most were heteromodal. These heteromodal regions included posterior midline structures such as the posterior cingulate/precuneus, which play an important role in maintaining consciousness.[27,28] Results from studies of functional connectivity (including the current study) indicate that both corticocortical and thalamocortical connectivity decreases during slow wave sleep.[11,23,24] It may be that the decrease in thalamocortical connectivity causes the decrease in corticocortical connectivity, and this decrease in turn underlies increased sensory awareness thresholds. That is, increased sensory awareness thresholds may occur because sensory information is not integrated among heteromodal cortical regions. This notion is consistent with the observation that in humans, changes in thalamic activity (as measured by depth EEG) during sleep precede changes in cortical activity[29] and differs from the hypothesis that sensory awareness thresholds are directly controlled by the thalamus. Instead, this notion suggests that selective decreases in functional connectivity of centromedian nucleus and heteromodal cortices underlie the attenuated downstream processing of intact sensory input that is behaviorally expressed as decreased higher-order awareness.

As discussed in a variety of contexts,[26] slow wave sleep represents a profound alteration in the level and content of consciousness, and a decrease in both corticocortical and thalamocortical connectivity is observed during slow wave sleep; similarly, a decrease in both corticocortical and thalamocortical connectivity is observed in anesthesia and coma.[30] The decreases in thalamocortical connectivity in such altered states of consciousness are mostly confined to heteromodal cortical regions such as the posterior cingulate/precuneus, which is similar to the current results. Therefore, changes in thalamocortical connectivity may serve as a universal control switch[31] that underlies changes in consciousness observed in coma, general anesthesia, and natural sleep.

Limitations

The participants in this study were sleep deprived in order to facilitate sleep inside the scanner. Sleep that follows sleep deprivation is quantitatively different from sleep following a single day of wakefulness, but it is not qualitatively different, so it is unlikely that sleep deprivation affected the basic relationships observed in the current study. Nevertheless, future studies should explore other methods to facilitate sleep inside the scanner.[32] It would also be important to measure thalamocortical connectivity during rested wakefulness and sleep deprived wakefulness because corticocortical connectivity changes during such a manipulation.[33] For the current study, given most of the epochs that were chosen for the wake condition occurred after the first slow wave sleep bout, the differences in connectivity that we observed may be specific to differences between sleep and postsleep wakefulness.

Given the size of the functional voxels relative to the size of the centromedian nucleus, it is possible that we had insufficient spatial resolution to differentiate individual thalamic nuclei. However, using a similar resolution, Zhang and colleagues and Zou and colleagues were able to differentiate individual thalamic nuclei.[34,35] Also, results from the supplementary analysis performed in the current study (in which the lateral geniculate nucleus was used as the seed region) showed that the whole-brain correlation pattern for the lateral geniculate nucleus was unique compared to the pattern for the centromedian nucleus. The unique pattern found for each seed region indicates that we were able to extract unique functional activity from each nucleus.

Other issues should also be considered in the context of comparing these two thalamic nuclei. Although we obtained similar temporal signal-to-noise ratios for each nucleus, it is still possible that signal-to-noise ratio differences in each nucleus could have caused differences in connectivity estimates. These signal-to-noise ratio differences could be due to minor differences in size or signal loss to magnetic field inhomogeneities.

Obtaining simultaneous EEG-fMRI data presents a number of technical challenges. One of these challenges is the acoustic noise generated by the MRI scanner.[32,36] As a result of the presence of this acoustic noise, the participants who successfully sleep during fMRI may not be representative of the general population. In addition to the challenges associated with simply initiating and maintaining sleep, the acoustic noise associated with fMRI may suppress certain stages such as REM sleep.[36]

A limitation of this study is its small sample size. This is due, in part, to the burdensome nature of conducting this type of research. Nevertheless, sleep neuroimagers have begun to increase their sample sizes, and it is important that this trend continues. Future studies should be designed to collect data from a very large number of subjects so that normative data can be obtained from those studies. Returning to the context of the current study, the results should be interpreted with caution until they are replicated. In addition to the possibility that the current results are spurious, it is also possible that some true effects were not detected. This limitation may be compounded by our use of multiple testing correction based on cluster size.

Future Work

The current results are relevant to studies in which event-related fMRI activity has been measured in response to subarousal-threshold stimuli during sleep. For example, Wehrle and colleagues[37] delivered subarousal-threshold auditory stimuli during tonic REM sleep (i.e., without concurrent eye movements) and during phasic REM sleep (i.e., with concurrent eye movements). Primary auditory cortex activity was observed during tonic REM but was reduced during phasic REM. Their results suggest decreased thalamocortical connectivity in phasic REM sleep, which could be directly determined via thalamic connectivity analyses similar to those used in the current study. Based on the current results, it would be predicted that thalamocortical connectivity with nonspecific nuclei is reduced during phasic REM (similar to reduced connectivity

seen during slow wave sleep), whereas thalamocortical connectivity with relay nuclei would not be different from that seen during wakefulness.

Finally, it may also be worthwhile to measure thalamocortical connectivity during sleep in patients with parasomnias such as sleepwalking. Brain activity during sleepwalking is characterized by increases in the cingulate cortex and decreases in the frontoparietal regions. It has been suggested that these differences represent a dissociation between thalamocortical connectivity in the cingulate cortex and thalamocortical connectivity in other cortical regions.[38] This hypothesis could be tested directly using measures of functional connectivity with single-photon emission computed tomography data.

ACKNOWLEDGMENTS

Dante Picchioni is at the National Institutes of Health. Morgan L. Pixa is at Virginia Polytechnic Institute and State University. Masaki Fukunaga is at Osaka University. Walter S. Carr is at the Walter Reed Army Institute of Research. Silvina G. Horovitz is at the Human Motor Control Section at the National Institute of Neurological Disorders and Stroke.

DISCLOSURE STATEMENT

This was not an industry supported study. This work was supported by the Intramural Program of the National Institute on Deafness and Other Communication Disorders, the Intramural Program of the National Institute of Neurological Disorders and Stroke, the National Academy of Sciences-National Research Council Postdoctoral Research Associateship Program, and the US Army Military Operational Medicine Research Program. The views expressed in this article are those of the authors and do not reflect the official policy or position of the Department of the Army, the Department of the Navy, the Department of Defense, the Department of Health and Human Services, the National Institutes of Health, the US Government, or any of the institutions with which the authors are affiliated. LCDR Carr is a military service member, and this work was prepared as part of his official duties. Title 17 U.S.C. §105 provides that "Copyright protection under this title is not available for any work of the United States Government." Title 17 U.S.C. §101 defines a US Government work as a work prepared by a military service member or employee of the US Government as part of that person's official duties. The authors have indicated no financial conflicts of interest.

REFERENCES

1. Jones, EG. The anatomy of sensory relay functions in the thalamus. Prog Brain Res 1991;87:29-52.
2. Llinas RR, Steriade M. Bursting of thalamic neurons and states of vigilance. J Neurophysiol 2006;95:3297-308.
3. Van der Werf YD, Witter MP, Groenewegen HJ. The intralaminar and midline nuclei of the thalamus. Anatomical and functional evidence for participation in processes of arousal and awareness. Brain Res Brain Res Rev 2002;39:107-40.
4. Rechtschaffen A, Hauri P, Zeitlin M. Auditory awakening thresholds in REM and NREM sleep stages. Percept Mot Skills 1966;22:927-42.
5. Steriade M, Deschenes M, Domich L, Mulle C. Abolition of spindle oscillations in thalamic neurons disconnected from nucleus reticularis thalami. J Neurophysiol 1985;54:1473-97.
6. Steriade M, McCormick DA, Sejnowski TJ. Thalamocortical oscillations in the sleeping and aroused brain. Science 1993;262:679-85.
7. Timofeev I, Contreras D, Steriade M. Synaptic responsiveness of cortical and thalamic neurones during various phases of slow sleep oscillation in cat. J Physiol 1996;494:265-78.
8. Blake H, Gerard RW. Brain potentials during sleep. Am J Physiol 1937;119:692-703.
9. Laufs H, Walker MC, Lund TE. 'Brain activation and hypothalamic functional connectivity during human non-rapid eye movement sleep: an EEG/fMRI study'--its limitations and an alternative approach. Brain 2007;130:e75.
10. Spoormaker VI, Schroter MS, Gleiser PM, et al. Development of a large-scale functional brain network during human non-rapid eye movement sleep. J Neurosci 2010;30:11379-87.
11. Horovitz SG, Braun AR, Carr WS, et al. Decoupling of the brain's default mode network during deep sleep. Proc Natl Acad Sci U S A 2009;106:11376-81.
12. Picchioni D, Horovitz SG, Fukunaga M, et al. Infraslow EEG oscillations organize large scale cortical-subcortical interactions during sleep: a combined EEG/fMRI study. Brain Res 2011;1374:63-72.
13. Allen PJ, Josephs O, Turner R. A method for removing imaging artifact from continuous EEG recorded during functional MRI. Neuroimage 2000;12:230-9.
14. Srivastava G, Crottaz-Herbette S, Lau KM, Glover GH, Menon V. ICA-based procedures for removing ballistocardiogram artifacts from EEG data acquired in the MRI scanner. Neuroimage 2005;24:50-60.
15. Rechtschaffen A, Kales A. A manual of standardized terminology, techniques, and scoring system for sleep stages of human subjects. Los Angeles: Brain Research Institute, 1968.
16. de Zwart JA, Ledden PJ, van Gelderen P, Bodurka J, Chu R, Duyn JH. Signal-to-noise ratio and parallel imaging performance of a 16-channel receive-only brain coil array at 3.0 T. Magn Reson Med 2004;51:22-6.
17. Jezzard P, Balaban RS. Correction for geometric distortion in echo planar images from B0 field variations. Magn Reson Med 1995;34:65-73.
18. Glover GH, Li TQ, Ress D. Image-based method for retrospective correction of physiological motion effects in fMRI: RETROICOR. Magn Reson Med 2000;44:162-7.
19. Shmueli K, van Gelderen P, de Zwart JA, et al. Low-frequency fluctuations in the cardiac rate as a source of variance in the resting-state fMRI BOLD signal. Neuroimage 2007;38:306-20.
20. Mai JK, Paxinos G, Voss T. Atlas of the human brain (3rd ed.). Amsterdam: Academic Press, 2007.
21. Borbely AA, Strauch I, Baumann F, Brandeis D, Lehmann D. Sleep deprivation: effect on sleep stages and EEG power density in man. Electroencephalogr Clin Neurophysiol 1981;51:483-93.
22. Lancaster JL, Woldorff MG, Parsons LM, et al. Automated Talairach atlas labels for functional brain mapping. Hum Brain Mapp 2000;10:120-31.
23. Koike T, Kan S, Misaki M, Miyauchi S. Connectivity pattern changes in default-mode network with deep non-REM and REM sleep. Neurosci Res 2011;69:322-30.
24. Samann PG, Wehrle R, Hoehn D, et al. Development of the brain's default mode network from wakefulness to slow wave sleep. Cereb Cortex 2011;21:2082-93.
25. Massimini M, Ferrarelli F, Huber R, Esser SK, Singh H, Tononi G. Breakdown of cortical effective connectivity during sleep. Science 2005;309:2228-32.
26. Tononi G. Consciousness, information integration, and the brain. Prog Brain Res 2005;150:109-26.
27. Gusnard DA, Raichle ME. Searching for a baseline: functional imaging and the resting human brain. Nat Rev Neurosci 2001;2:685-94.
28. Vogt BA, Laureys S. Posterior cingulate, precuneal and retrosplenial cortices: cytology and components of the neural network correlates of consciousness. Prog Brain Res 2005;150:205-17.
29. Magnin M, Rey M, Bastuji H, Guillemant P, Mauguiere F, Garcia-Larrea L. Thalamic deactivation at sleep onset precedes that of the cerebral cortex in humans. Proc Natl Acad Sci U S A 2010;107:3829-33.
30. Noirhomme Q, Soddu A, Lehembre R, et al. Brain connectivity in pathological and pharmacological coma. Front Syst Neurosci 2010;4:160.
31. Franks NP. General anaesthesia: from molecular targets to neuronal pathways of sleep and arousal. Nat Rev Neurosci 2008;9:370-86.
32. Duyn JH. EEG-fMRI methods for the study of brain networks during sleep. Front Neurol 2012;3:100.
33. Gujar N, Yoo SS, Hu P, Walker MP. The unrested resting brain: sleep deprivation alters activity within the default-mode network. J Cogn Neurosci 2010;22:1637-48.

34. Zhang D, Snyder AZ, Fox MD, Sansbury MW, Shimony JS, Raichle ME. Intrinsic functional relations between human cerebral cortex and thalamus. J Neurophysiol 2008;100:1740-8.
35. Zou Q, Long X, Zuo X, et al. Functional connectivity between the thalamus and visual cortex under eyes closed and eyes open conditions: a resting-state fMRI study. Hum Brain Mapp 2009;30:3066-78.
36. Czisch M, Wehrle R. Sleep. In: Mulert C, Lemieux L, eds. EEG-fMRI: physiological basis, technique, and applications. Berlin: Springer, 1983:279-305.
37. Wehrle R, Kaufmann C, Wetter TC, et al. Functional microstates within human REM sleep: first evidence from fMRI of a thalamocortical network specific for phasic REM periods. Eur J Neurosci 2007:25:863-71.
38. Bassetti C, Vella S, Donati F, Wielepp P, Weder B. SPECT during sleepwalking. Lancet 2000;356:484-5.